Evaluation of a Proposed Inverted U-Shaped Retaining Wall

Mur de soutènement en forme de U inverse

Ahmed El-Orabi

Geotechnical Engineer, Dar Al-Handasah, Egypt, ahmed.orabi@dar.com

Rami M. El-Sherbiny

Associate Professor, Faculty of Engineering, Cairo University, Egypt, rsherbiny@eng.cu.edu.eg

Abdelsalam A. Salem

Professor, Faculty of Engineering, Cairo University, Egypt, salemconsult@a-salem.com

ABSTRACT: This paper presents a proposed U-shaped wall configuration that provides an alternative to gravity wall system in areas with limited base width. The inverted U-wall is a monolithic reinforced concrete frame, which is composed of a stem with limited embedment, relief floor/slab, and a dead-man. The stem extends from the toe of the wall to an intermediate height of the total retained height. A short gravity wall is constructed on top of the U-shaped wall to the top of the retained height. The purpose of the paper is to study the performance of the proposed wall system in terms of global stability, induced straining actions, and wall movements. The different aspects of wall geometry are investigated by conducting a comprehensive parametric study using 2-D limit equilibrium and 2-D finite element analyses. The effect of wall height, stem height, embedment depth, floor length, and dead-man height are investigated. The analyses indicate a satisfactory performance of the proposed inverted U-wall configuration in terms of stability and serviceability. The utilization of the relief floor contributes to reducing the earth pressure on the wall stem. The floor also acts as a tie to the dead-man, which contributes to the overall stability of the wall.

RÉSUMÉ: Cet article présente une configuration de projet mur en forme de U qui offre une alternative au système de mur de gravité dans les zones largeur base limitée. La paroi U inversée est une trame monolithiques en béton armé, qui se compose d'une tige avec un enfoncement limité, secours/dalle de plancher et un homme mort. La tige s'étend de l'orteil du mur à une hauteur intermédiaire de la hauteur totale de rétention. Un mur de gravité court est construit par-dessus le mur en U vers le haut de la hauteur retenue. Le but du document est d'étudier les performances du système en termes de stabilité mondiale, les actions de serrage induites et mouvements du mur proposée. Les différents aspects de la géométrie du mur sont soigneusement étudiés par menée une étude paramétrique complet à l'aide d'éléments finis 2D et analyses d'équilibre limite 2D. L'effet de la hauteur du mur, hauteur de tige, profondeur d'encastrement, dalle longueur et hauteur de corps-mort sont l'objet d'une enquête. Les analyses indiquent un rendement satisfaisant de la configuration proposée de la paroi U inversé en termes de stabilité et facilité d'entretien. L'utilisation de la dalle de secours contribue à réduire la pression des terres sur la tige de la paroi, qui peut entraîner des matériaux et réduction des coûts. La dalle agit aussi comme un lien avec l'homme mort qui contribue à la stabilité globale du mur.

KEYWORDS: Retaining wall, Inverted U-shaped wall, Relief floor, Dead-man, Finite element analysis.

1 INTRODUCTION

Gravity type retaining walls have been traditionally used as retaining structures in fill areas. However, the footprint of gravity walls amounts to 60% to 70% of the height, which may cause challenges in narrow areas with limited base width. Even with stabilized back-slopes, the width of narrow gravity walls including mechanically stabilized walls exceeds 30% of the height (Morrison et al. 2006, and Yang et al. 2011). The proposed inverted U-wall provides an alternative to gravity wall system in areas with base width limitations. Moreover, the proposed system may also provide cost benefit compared to cantilever or counterfort gravity-type retaining walls. The inverted U-Shape reinforced-concrete wall consists of a stem embedded at the toe and extending to an optimized intermediate height, a relief floor acting as a tie-back, a dead-man, and a limited height gravity wall extending above the stem for the remaining wall height (Fig. 1). The relief floor is monolithically cast with the top of the stem and dead-man. Thus, overburden vertical loads are transferred to the two vertical members. Strip foundations are used underneath the stem and dead-man to reduce stress concentration at the toes. The gravity type wall at the top provides an economic solution for the remaining height while allowing for embedment of the dead-man and relief floor.

The principal of utilizing a relief floor was developed by Vandepitte (1979) in association with a gravity type retaining wall. The introduction of a relief floor rigidly fixed to the wall resulted in increasing the stabilizing moment against overturning, reducing the earth pressure on the wall, and reducing the eccentricity on the base. Vandepitte introduced an analytical approach to calculate the reduction in earth-pressure on the wall due to stress redistribution below the relief floor. Ganne & Raucroix (2013) performed finite element analysis of a gravity-type inverted-T cantilever wall with a relief floor and found good agreement between the resulting earth pressure and that calculated using Vandepitte's analytical approach.

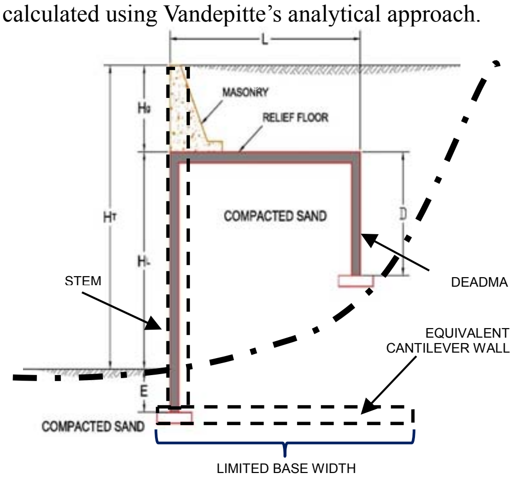

Figure 1. Inverted U-wall retaining wall

The proposed inverted U-wall combines the advantages of the relief floor with a dead-man at the back that contributes to the stability and serviceability of the wall. The purpose of this paper is to assess the global stability of the proposed inverted U-wall; and to evaluate wall movements, induced bending moments, and member forces.

2 METHODOLOGY

Two-dimensional plane-strain finite element analyses were conducted using the software PLAXIS to evaluate wall stability, movements and induced straining actions of the inverted U-wall. The backfill and foundation soils were modeled as two-dimensional 15-node continuum elements using the hardening soil model, HSM (Brinkgreve et al. 2002). The HSM is a non-linear elasto-plastic model capable of accounting for stress dependency of the soil stiffness in loading and unloading conditions. Typical dense sand properties were adopted to represent the compacted replacement soil surrounding the wall. The natural soils in such wall conditions with stable back-slopes are typically strong competent soils. Thus, the foundation soil was also modeled as a sandy soil.

The proposed inverted U-wall system was modeled as a reinforced concrete section of thickness ranging between 40cm and 60cm using isotropic elastic plate elements. Interface elements were utilized at the soil/wall interface and at the gravity wall/relief floor interface. The interface is modeled as a linear elastic perfectly plastic element with a reduction factor (R_{inter}) that relates the interface strength to the adjacent soil strength. A surcharge load of 10 kPa was applied at the top of the wall. A summary of the utilized material properties is provided in Table 1. A typical FE model showing the various components and the generated mesh is shown in Figure 2.

Table 1. Adopted soil/concrete parameters in FEM

Parameters	SAND Foundation	SAND Backfill	Concrete
Model	HSM	HSM	Linear-Elastic
Drainage type	Drained	Drained	Non-porous
γ_{sat} (kN/m^3)	19	20	23
E_{50}^{ref} (MPa)	40	50	-
E_{oed}^{ref} (MPa)	40	50	-
E_{ur}^{ref} (MPa)	120	150	-
E_{ref} (MPa)	-	-	29000
m	0.5	0.5	-
c´ (kPa)	2	2	-
ϕ´	34	36	-
ν_{ur}, ν	0.2	0.2	0.15
ψ	4	6	-
R_{inter}	0.85	0.85	1

Bottom-up construction is most appropriate for construction of the proposed inverted U-wall. A strutting system is required during construction of the wall to maintain stability until the backfilling is completed. The strut elements were modeled as a linear elastic “anchor” (Brinkgreve et al. 2002) assumed to have stiffness (EA) of 47 MN.

The finite element modeling sequence followed the proposed construction sequence. An initially flat ground level is assumed in the analysis. This configuration is more conservative than assuming a stable back slope due to higher induced earth pressures. The braced inverted U-shaped wall, backfill soil and the gravity wall are activated together. The displacements were reset to zero at this stage then the strutting system was removed in stages from bottom to top and the surcharge load is applied.

A final phi-c reduction (Brinkgreve et al. 2002) stage is performed to calculate the global stability safety factor. Two dimensional limit equilibrium (LE) analyses are also conducted using SLIDE software to evaluate global stability factor of safety. Non-circular slip surfaces are adopted in the limit equilibrium analysis to accommodate the wall geometry complexity. Spencer’s method (Spencer, 1967) method was employed to accommodate force and moment equilibrium.

The numerical model of the proposed U-shaped wall was validated against the analytical approach developed by Vandepitte (1979). The earth pressure (E.P.) distribution was found to be closer to the active E.P. calculated using Rankine’s approach directly below the relief floor for the case of no vertical stress transfer, then increases gradually to approach the active earth pressure considering full vertical stress transfer (Fig. 3). The E.P. distribution acting on the wall underneath the relief floor resulting from the FEA was in good agreement with the E.P. calculated analytically as shown in Figure 3.

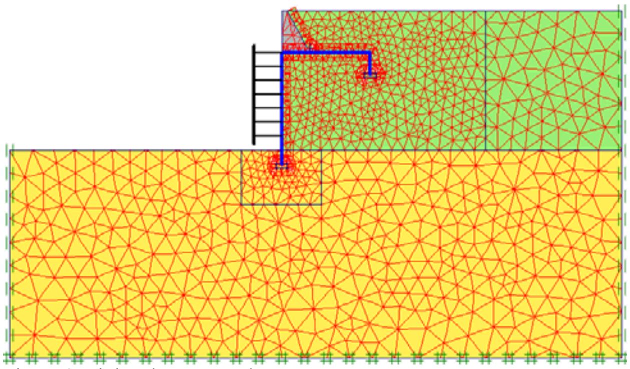

Figure 2. Finite element mesh

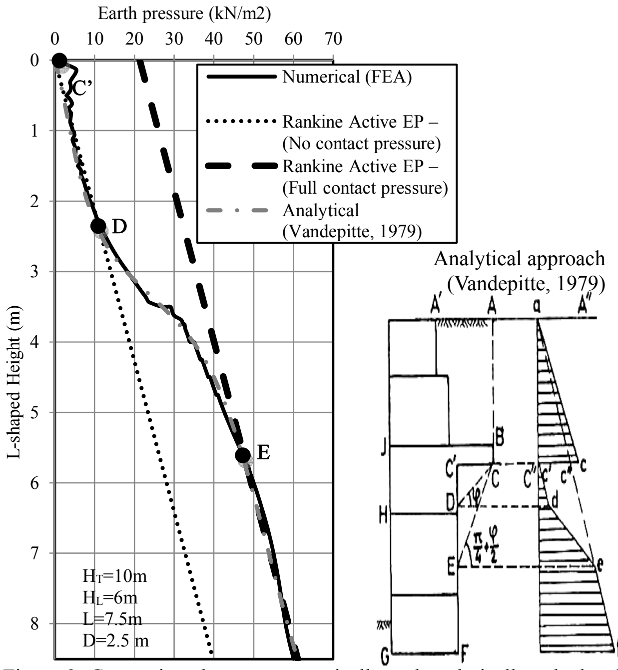

Figure 3. Comparison between numerically and analytically calculated earth pressures below the relief floor.

3 RESULTS & ANALYSIS

Model walls having a total height (H_T) of 7 m, 10 m, and 13 m were investigated as part of this study with embedment of 1 m and 2 m (El-Orabi, 2017). This paper presents the results of a model wall having (H_T) of 10 m and (E) of 1.0 m. The analyses presented herein consider the variation in exposed height (H_L) as a normalized ratio (H_L/H_T) values of 0.5, 0.6 and 0.7. The relief floor length is normalized as a ratio (L/H_L) and varied having values of 0.9, 1.1, 1.3 and 1.5. In addition, the dead-man depth (D) is normalized as a ratio (D/H_L) and varied having values of 0, 0.2, 0.4, and 0.6. The following sections presents the effect of varying wall geometry on the factor of safety (FS), wall movements and induced straining actions.

3.1 *Factor of safety (FS)*

The global stability FS was assessed using LE and FE analyses. The resulting failure surfaces were in good agreement, while resulting FS from FEA were consistently lower by 2% to

8%. A typical output from the FEA showing induced shear strains along the failure surface at the end of phi-c reduction stage is presented in Figure 4. The results show the critical failure surface forming an active wedge against the dead-man, and a passive wedge against the stem with the surface intersecting both toes at points of high shear strains. Shear stress concentrations at the toes of the stem and dead-man may be the cause of the lower FS from the FEA. It is also evident that a gap occurs between the relief floor and the underlying soil, which explains the reduction in lateral E.P. acting at the top of the stem.

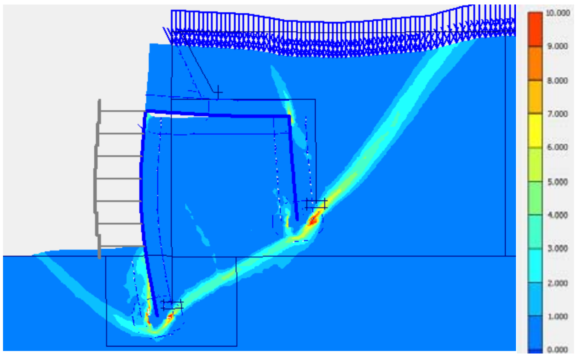

Figure 4. Typical shear strains at the end of phi-c reduction stage

Effect of Relief Floor Length (L) & Dead-Man Depth (D): The proposed wall was evaluated without a dead-man (D/H_L=0.0) in order to investigate the effect of (L) on the FS at (H_L/H_T) of 0.7 (Fig. 5). The FS did not significantly increase with increasing (L/H_L) from 0.9 to 1.5. Further increase in (L) is considered impractical. However, introducing a dead-man having (D/H_L) of 0.4 or greater was more effective in increasing the FS. Increasing (D/H_L) from 0 to 0.6 resulted in 15% increase in FS at (L/H_L) of 0.9 and 35% increase in FS at (L/H_L) of 1.5. Thus, the influence of increasing (D/H_L) was more significant at higher (L/H_L). A combined configuration of (D/H_L) and (L/H_L) within the investigated range of values can be used to achieve acceptable target factors of safety in the range of 1.25 to 1.5.

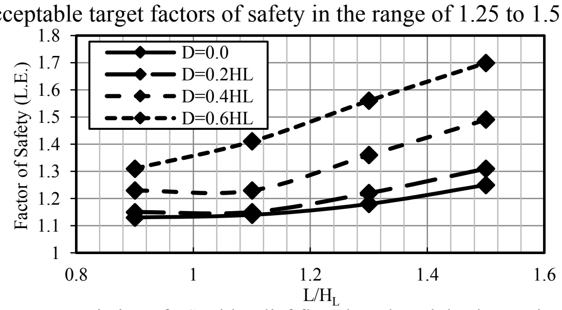

Figure 5. Variation of FS with relief floor length and dead-man depth at (H_L/H_T) of 0.7.

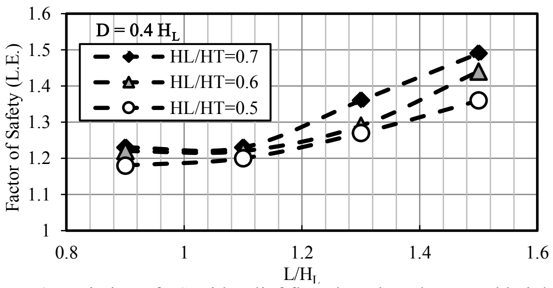

Figure 6. Variation of FS with relief floor length and exposed height.

Effect of Burial Ratio (H_L/H_T): Analyses were conducted considering (H_L/H_T) ratios of 0.5, 0.6 and 0.7 for variable (L/H_L) and (D/H_L) of 0.4 (Fig. 6). The ratios were selected to limit the height of the top gravity wall to a cost effective height for the (H_T) range investigated. As the buried depth decreases (i.e. H_L/H_T increases), the F.S. increases. The FS increase ranged from 5% at (L/H_L) of 0.9 to 10% at (L/H_L) of 1.5.

3.2 *Wall movements*

The maximum horizontal wall movements were observed to occur within the vicinity of the middle of the exposed height (H_L), while maximum vertical surface settlements occurred above the dead-man (Fig. 4). The maximum vertical movements underneath the relief floor occurred underneath the gravity wall. The maximum horizontal and vertical deformations were observed for the range of investigated (L/H_L), (D/H_L), and (H_L/H_T).

Effect of Relief Floor Length (L) & Dead-Man Depth (D): The wall movements at different ratios of (L/H_L) and (D/H_L) are presented in Figure 7. It is observed that the vertical and horizontal wall movements decrease with increasing (L/H_L). The introduction of the shortest dead-man (D/H_L = 0.2) significantly decreases wall movements, with more significant influence at lower (L/H_L) ratios. Further increase in (D/H_L) has a less significant effect on movements. Introducing the dead-man resulted in up to 35 % reduction in horizontal deflections and up to 50% reduction in vertical settlements.

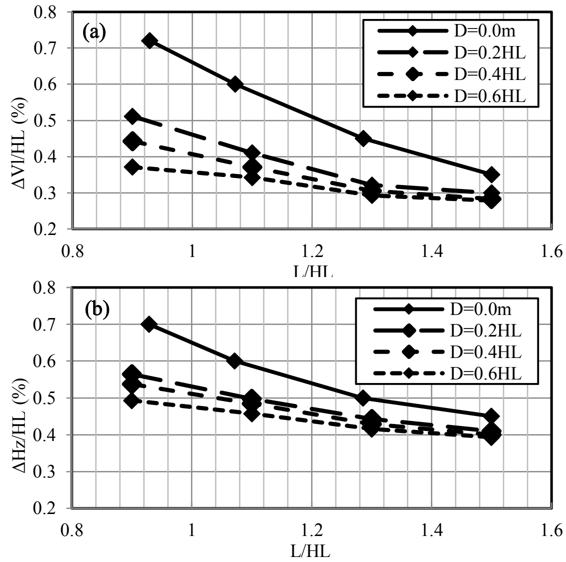

Figure 7. Maximum wall movements at (H_L/H_T) of 0.7; (a) maximum vertical movements, (b) maximum horizontal movements

Effect of Burial Ratio (H_L/H_T): A comparison between wall movements at different ratios of buried depth is presented in Figure 8. Vertical and horizontal wall movements significantly decrease (up to 50%) as the buried depth decreases (i.e. H_L/H_T increases), with more pronounced effect at lower (L/H_L) values. As the buried depth increases the vertical stress applied on the relief floor increases linearly and results in increasing wall movements. This further emphasizes the importance of reducing the buried depth for safety and serviceability purposes.

3.3 *Wall straining actions*

Induced straining actions in the concrete frame of the inverted U-wall govern the wall design cross section and reinforcement. The induced maximum bending moment (BM) on the frame and maximum tension force (T) in the relief floor were therefore investigated. Only the maximum envelope of the straining actions from all construction stages is considered. Maximum (BM) occur at the connection of the stem and relief floor, and mid-span of the relief floor. Maximum (T) occur in the relief floor while the stem and dead-man were under compression.

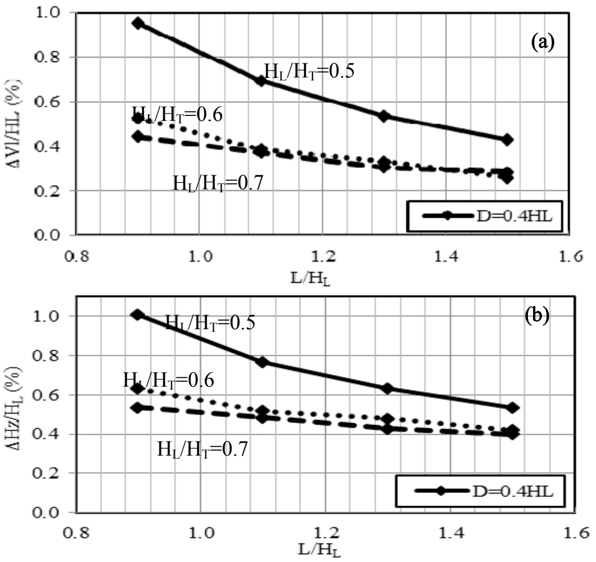

Figure 8. Maximum wall movements at (D/H_L) of 0.4; (a) maximum vertical movements, (b) maximum horizontal movements

<u>Effect of Relief Floor Length (L) & Dead-Man Depth (D):</u> The effect of increasing (L/H_L) and (D/H_L) on straining actions is presented in Figures 9 and 10. The effect of increasing (L/H_L) on maximum (BM) is minor in absence of a dead-man, and resulted in an increase of up to 15 % in maximum (BM) in presence of a dead-man. Similarly, the induced maximum (T) in the relief floor increases approximately linearly as the relief floor length increases. Utilizing the dead man segment increases the maximum (T) by 15% at high (L/H_L) to 75% at low (L/H_L), compared to the case of no dead-man.

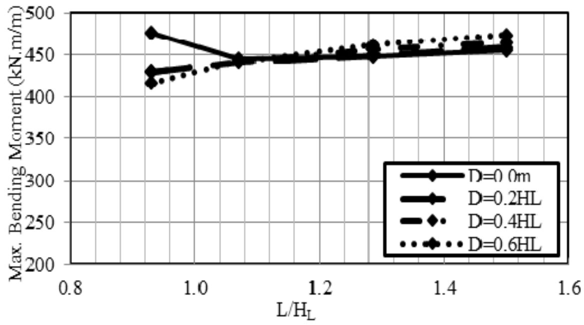

Figure 9. Maximum bending moment (envelope) for a buried ratio (H_L/H_T) of 0.7.

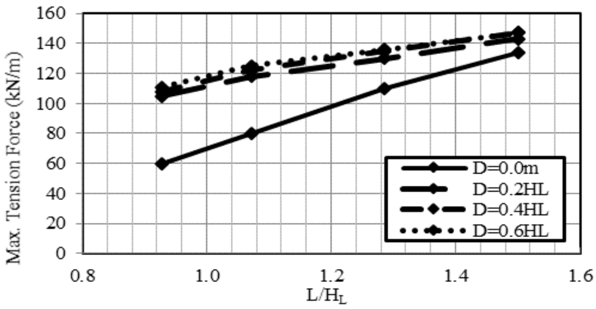

Figure 10. Maximum tension force (envelope) in the relief floor for a buried ratio (H_L/H_T) of 0.7.

<u>Effect of Burial Ratio (H_L/H_T):</u> Figures 11 and 12 present a comparison between the maximum induced straining actions in case of employing different ratios of buried depth. The level where the relief floor is utilized is of great influence on the induced staining actions (Figs. 11 & 12). Changing (H_L/H_T) from 0.5 to 0.7 (from deeper to shallower depth) would increase the moment arm. Accordingly, larger BMs are induced. Furthermore, placing the relief floor deeper results in linear increase of the passive thrust behind dead man, which leads to a larger maximum induced (T) on the relief floor.

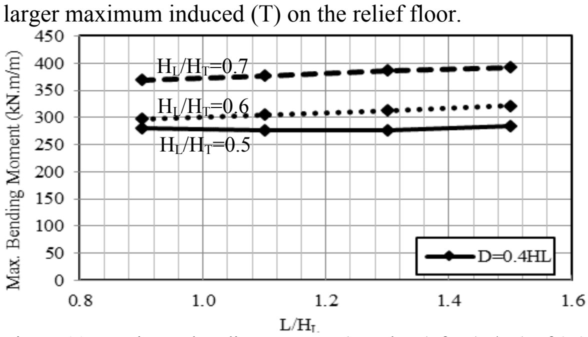

Figure 11. Maximum bending moment (envelope) for (D/H_L) of 0.4 and variable buried ratios.

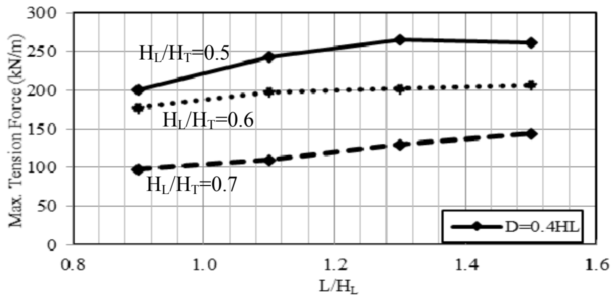

Figure 12. Maximum tension force (envelope) in the relief floor (envelope) for (D/HL) of 0.4 and variable buried ratios.

4 CONCLUSION

The following conclusions are drawn from this research:

- Satisfactory performance of the inverted U-wall in terms of stability and serviceability is achievable.
- Utilization of relief floor contributes to reducing the earth pressure on the stem, which results in material and cost saving. The relief floor also acts as a tie to the dead-man.
- Utilization of the dead-man highly contributes to increasing wall stability and serviceability, which provides an added advantage over conventional relief floors.
- The wall stability is governed by height of the stem, length of the relief floor, and depth and height of the dead-man.
- Deformations are highly reduced and tension forces in relief floor increase in presence of a dead-man, while being less sensitive to the height of dead-man and length of relief floor.
- Bending moments are not significantly affected by the dead-man and relief floor configuration.
- As the buried depth increases, the FS and BM decrease, while deformations and tension in relief floor increase.

5 REFERENCES

Brinkgreve, R.B.J., Broere, W., and Waterman, D. 2002. PLAXIS V8 Reference Manual. PLAXIS b.v., Netherlands.

El-Orabi, A. 2017. Performance of Inverted U-Shaped Retaining Wall. M.Sc. Thesis, Faculty of Engineering, Cairo University, Egypt.

Ganne, P.P., and Raucroix, X. 2013. Design of Inverted T-shaped Cantilever Wall with a Relief Floor. 18th Int'l Conference on Soil Mechanics & Geotechnical Engineering, France, September.

Morrison, K., Harrison, F., Collin, J. G., Dodds, A., and Arndt, B. 2006. Shored mechanically stabilized earth (SMSE) wall systems design guidelines. Rep. No. FHWA-CFL/TD-06-001,Washington, DC.

Spencer, E. (1967). "A Method of Analysis of the Stability of Embankments Assuming Parallel Inter-Slice Forces," Geotechnique, 17 (1), pp. 11-26.

Vandepitte D. 1979. Berekening van constructies. Scientia, Genth. (in Dutch).

Yang, K., Ching, J., Zornberg, J. 2011. Reliability-Based Design for External Stability of Narrow Mechanically Stabilized Earth Walls: Calibration from Centrifuge Tests. J. Geot. & Geoenv. Eng. 137(3).